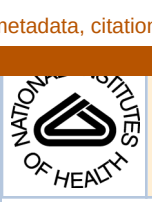

Published in final edited form as:
Pharm Res. 2010 September ; 27(9): 1987–1998. doi:10.1007/s11095-010-0203-x.

Evaluation of ^{99m}Technetium-Mebrofenin and ^{99m}Technetium-Sestamibi as Specific Probes for Hepatic Transport Protein Function in Rat and Human Hepatocytes

Brandon Swift, **Wei Yue**, and **Kim L. R. Brouwer***
Division of Pharmacotherapy and Experimental Therapeutics, UNC Eshelman School of Pharmacy, University of North Carolina at Chapel Hill, Chapel Hill, North Carolina, 27599-7569

Abstract

Purpose—This study characterized ^{99m}Tc-Mebrofenin (MEB) and ^{99m}Tc-Sestamibi (MIBI) hepatic transport and preferential efflux routes (canalicular vs. basolateral) in rat and human sandwich-cultured hepatocytes (SCH).

Methods—^{99m}Tc-MEB and ^{99m}Tc-MIBI disposition was determined in suspended hepatocytes and in SCH in the presence and absence of inhibitors and genetic knockdown of breast cancer resistance protein (Bcrp).

Results—The general organic anion transporting polypeptide (Oatp/OATP) inhibitor rifamycin SV reduced initial ^{99m}Tc-MEB uptake in rat and human suspended hepatocytes. Initial ^{99m}Tc-MIBI uptake in suspended rat hepatocytes was not Na^+-dependent or influenced by inhibitors. Multidrug resistance-associated protein (Mrp2/MRP2) inhibitors decreased ^{99m}Tc-MEB canalicular efflux in rat and human SCH. ^{99m}Tc-MEB efflux in human SCH was predominantly canalicular (45.8±8.6%), and ~3-fold greater than in rat SCH. ^{99m}Tc-MIBI canalicular efflux was similar in human and rat SCH; basolateral efflux was 37% greater in human than rat SCH. ^{99m}Tc-MIBI cellular accumulation, biliary excretion index and *in vitro* biliary clearance in rat SCH were unaffected by Bcrp knockdown.

Conclusion—^{99m}Tc-MEB hepatic uptake is predominantly Oatp-mediated with biliary excretion by Mrp2. ^{99m}Tc-MIBI appears to passively diffuse into hepatocytes; biliary excretion is mediated by P-gp. The SCH model is useful to investigate factors that may alter the route and/or extent of hepatic basolateral and canalicular efflux of substrates.

Keywords

^{99m}Technetium-Mebrofenin; ^{99m}Technetium-Sestamibi; Sandwich-Cultured Hepatocytes; Hepatic Basolateral Efflux; Hepatic Canalicular Efflux

Introduction

Probe substrates are used to obtain an *in vivo* phenotypic measure of specific biotransformation or transport pathways in preclinical or clinical species. Ideally, a transport probe substrate would be specific for a single transport protein, relatively safe for healthy human volunteer studies and metabolically stable. There are currently very few identified transport probe substrates suitable for clinical use. Digoxin has been recommended as a P-

Corresponding author. Reprint Requests: UNC Eshelman School of Pharmacy, The University of North Carolina at Chapel Hill, 311 Pharmacy Lane, CB#7569, 3205 Kerr Hall, Chapel Hill, NC 27599-7569. Tel: (919)962-7030. Fax: (919)962-0644. kbrouwer@unc.edu.

glycoprotein (P-gp) probe in the FDA guidance (http://www.fda.gov/Cder/drug/drugInteractions/default.htm), however, digoxin also is transported by organic anion transporting polypeptides OATP1B3 and OATP4C1. ^{99m}Technetium-mebrofenin (^{99m}Tc-MEB) and ^{99m}Technetium-sestamibi (^{99m}Tc-MIBI) are candidate probe substrates for multidrug resistance associated protein 2 (MRP2) and P-gp, respectively.

^{99m}Tc-MEB is the ^{99m}Tc-labeled trimethylbromo analogue of acetanilidoiminodiacetic acid commonly used in nuclear medicine for hepatobiliary scintigraphy and evaluation of gallbladder dysfunction(1). This compound belongs to a class of agents that couples a lidocaine-like structure, resulting in high liver extraction, with ^{99m}technetium, which is ideal for gamma scintigraphy(2). Several hepatic transport proteins involved in the hepatobiliary disposition of ^{99m}Tc-MEB were characterized recently in expressed systems including OATP1B1, OATP1B3, MRP2 and MRP3(3). ^{99m}Tc-MEB exhibited increased and prolonged hepatic exposure measured by gamma scintigraphy in Mrp2-deficient TR$^-$ rats compared to WT rats, suggesting that Mrp2 is involved in canalicular transport(4). Furthermore, case reports have documented a failure to visualize the hepatobiliary tree after administration of ^{99m}Tc-disofenin (DISIDA), the diisopropyl analogue of acetanilidoiminodiacetic acid, when administered to patients with Dubin-Johnson syndrome (MRP2-deficiency)(5). More than 98% of a ^{99m}Tc-MEB dose is taken up by the liver; the hepatic excretion half-life of ^{99m}Tc-MEB is rapid (16min) and ~1.5% of the dose was recovered in urine after 24 hours in humans(2).

^{99m}Tc-MIBI, a monovalent cation complex of ^{99m}Tc (^{99m}Tc-2-methoxyisobutylisonitrile), is used clinically to assess myocardial perfusion; ^{99m}Tc-MIBI distributes into the heart in proportion to blood flow and myocardial viability(6, 7). Decreased uptake of ^{99m}Tc-MIBI in resistant cells also has been attributed to a lower membrane potential and reduced mitochondrial density(8). Several groups have used ^{99m}Tc-MIBI as a functional P-gp probe substrate in rodents and humans(9–12). Further investigations using cancer cells in culture revealed that ^{99m}Tc-MIBI is a MRP1 substrate (13). In TR$^-$ rats, ^{99m}Tc-MIBI cumulative recovery in bile, and liver activity profiles based on *in vivo* imaging, were similar compared to WT rats, suggesting that Mrp2 is not involved, or other mechanisms compensate for impaired hepatic excretion (14). In humans, ^{99m}Tc-MIBI undergoes renal elimination and fecal clearance mediated by biliary excretion and possibly intestinal secretion [Cardiolite® package insert;(3)].

^{99m}Tc-MIBI and analogs of ^{99m}Tc-MEB have been used as probe substrates to assess interindividual variation in hepatic drug disposition(10, 15, 16). Coadministration of ^{99m}Tc-MIBI with the P-gp inhibitors PSC833 and LY335979 resulted in prolonged hepatic exposure(9, 11, 12). ^{99m}Tc-MIBI pharmacokinetics were altered in a cohort of cancer patients with common single nucleotide polymorphisms (SNPs) in *ABCB1* exons 12 (C1236T) and 26 (C3435T); the elimination rate constant was significantly decreased(10). However, the mechanisms of ^{99m}Tc-MIBI hepatic transport have not been investigated fully, including potential compensatory proteins involved in hepatobiliary disposition. The purpose of the current study was to characterize the mechanisms of ^{99m}Tc-MEB and ^{99m}Tc-MIBI uptake and excretion in rat and human hepatocytes. The processes involved in hepatic uptake, basolateral efflux and canalicular excretion are too complicated to be completely elucidated *in vivo*. Therefore, suspended hepatocytes were used to investigate hepatic uptake mechanisms and sandwich-cultured hepatocytes (SCH) were used to elucidate the hepatic efflux of ^{99m}Tc-MEB and ^{99m}Tc-MIBI. TR$^-$ rats serve as a useful tool to examine altered hepatobiliary disposition in response to impaired Mrp2 function, and facilitate the identification of compensatory basolateral and apical efflux mechanisms involved in ^{99m}Tc-MEB hepatobiliary disposition.

Material and Methods

Materials

Dulbecco's modified Eagle's medium (DMEM), insulin, MEM non-essential amino acids solution (100x), L-glutamine, insulin and penicillin G-streptomycin solution were purchased from Invitrogen (Carlsbad, CA). Estradiol-17-β-D-glucuronide (E217G), para-aminohippuric acid sodium salt (PAH), tetraethylammonium (TEA), rifamycin SV, glycyrrhizic acid, clonidine, desipramine, ketoprofen, fetal bovine serum (FBS), Triton X-100, dexamethasone, and Hanks' balanced salt solution (HBSS) modified with (H-1387) or without (H-4891) calcium chloride were obtained from Sigma-Aldrich (St. Louis, MO). Collagenase (type 1) was obtained from Worthington Biochemical Corporation (Freehold, NJ). BioCoat™ collagen I plates, Matrigel™ basement membrane matrix, and ITS+™ (insulin/transferrin/selenium) culture supplement were purchased from BD Biosciences Discovery Labware (Bedford, MA). Bicinchoninic acid (BCA) protein assay reagents and BSA for the protein assay standard were purchased from Pierce Chemical Co. (Rockford, IL). ^{99m}Tc-MEB and ^{99m}Tc-MIBI were purchased as sterile doses on the day of the experiment from Cardinal Health Nuclear Pharmacy (Research Triangle Park, NC). Ultima Gold™ XR scintillation cocktail, ^{3}H-PAH (3.28Ci/mmol) and ^{3}H-E217G (45.8Ci/mmol) were purchased from Perkin Elmer Life Sciences (Boston, MA). ^{14}C-TEA (55mCi/mmol) was purchased from American Radiolabeled Chemicals. MK-571 sodium salt was purchased from Cayman Chemical Co (Ann Arbor, MI). N-(4-[2-(1,2,3,4-tetrahydro-6,7-dimethoxy-2-isoquinolinyl)ethyl]-phenyl)-9,10-dihydro-5-methoxy-9-oxo-4-acridine carboxamide (GF120918) was a gift from GlaxoSmithKline (Research Triangle Park, NC). All other chemicals and reagents were of analytical grade and available from commercial sources.

Animals

Male Wistar WT rats (201–312g) from Charles River Laboratories, Inc. and Mrp2-deficient TR^{-} rats bred at the UNC (228–306g; breeding stock obtained from Dr. Mary Vore, University of Kentucky, Lexington, KY) were used for SCH studies. All animals acclimated for one week before experiments. Rats were housed in an alternating 12-h light and dark cycle with free access to water and food prior to surgery. All animal procedures complied with the guidelines of the Institutional Animal Care and Use Committee (UNC, Chapel Hill, NC).

Suspended Hepatocyte Isolation/Uptake Studies—Rat hepatocytes were isolated by a two-step collagenase perfusion method as described previously(17). Viability, as determined by trypan blue exclusion, was 90 to 95% (mean = 92%). CellzDirect, Life Technologies (RTP, NC) kindly provided freshly isolated human hepatocytes in suspension. Hepatocyte donors included a 60 yr old female Caucasian, and 63 and 69 yr old male Caucasians, with no recent history of smoking or alcohol use. Hepatocyte viability, as determined by trypan blue exclusion, was 90, 86 and 89%, respectively. Isolated hepatocytes were suspended at 1×10^{6}cells/ml in cold modified Hank's buffer with 10mM Tris/5mM glucose (pH = 7.4) or Na^{+}-free choline buffer (10mM Tris, 5mM glucose, 5.4mM KCl, 1.8mM $CaCl_2$, 0.9mM $MgSO_4$, 10mM HEPES and 137mM choline; pH = 7.4) and stored on ice prior to conducting uptake studies(18). Hepatocyte suspensions were preincubated in bottom inverted Erlenmeyer flasks (rat) or 16×100mm glass vials (human) at 37 C for 5min; 0.1% DMSO or chemical inhibitor was added 1min before, followed by ^{99m}Tc-MEB (5μCi/mL), ^{99m}Tc-MIBI (5μCi/mL), ^{3}H-E217G (1μM, 60nCi/mL), ^{14}C-TEA (20μM, 60nCi/mL) or ^{3}H-PAH (0.2, 1 or 20μM, 60nCi/mL). The following concentrations of inhibitors were selected based upon reported affinities for the given active transport processes: 20μM rifamycin SV (Oatp1a1, Oatp1a4, OATP1B1, OATP1B3, and OATP2B1 inhibitor), 20μM glycyrrhizic acid (Oatp1a1, 1a4 and 1b2 inhibitor), 200μM clonidine [organic cation

transporter (Oct1) inhibitor], 10μM desipramine (Oct1 and 3 inhibitor), 5μM decynium 22 (OCT inhibitor), 10μM ketoprofen [organic anion transporter (Oat2) inhibitor]. Aliquots (100μL) of the suspension were removed at timed intervals (up to 5min), placed in 0.4-ml polyethylene tubes and centrifuged immediately through a top layer of silicone oil:mineral oil (82:18, v/v; 100μL) and a bottom layer of 3M KOH (50μL). ^{99m}Tc-MEB and ^{99m}Tc-MIBI in the cell pellet and supernatant were analyzed using a sodium iodide well counter and corrected for decay (^{99m}Tc $t_{1/2}$=6.01h). ^{3}H-E217G, ^{14}C-TEA or ^{3}H-PAH were analyzed by liquid scintillation counting. Adherent fluid volume was estimated with ^{14}C-inulin as described previously(19). Protein concentrations for individual hepatocyte suspensions were determined with the BCA protein assay reagent kit (Pierce) as instructed by the manufacturer. BSA, as supplied by the manufacturer, was used as a standard (0.2 – 1mg/mL).

Sandwich-Cultured Hepatocyte Studies—CellzDirect, Life Technologies (RTP, NC) provided human hepatocytes plated on six-well Biocoat™ plates and overlaid with Matrigel™. Hepatocyte donors were a 56 and 64 yr old female Caucasian with no history of smoking or alcohol use. Rat hepatocytes (>88% viability) were seeded [~1.5×10^6cells/well (TR^-) or 1.75×10^6cells/well (WT)] in 6-well BioCoat™ plates and overlaid with Matrigel™ basement membrane matrix as described previously(20). The culture medium was changed every 24h until experiments were performed on day 4 of culture.

Efflux Studies—On day 4, efflux experiments were performed as previously described(21) with modifications. Briefly, hepatocytes were rinsed with 2mL warm standard buffer and incubated with 1.5mL of ^{99m}Tc-MEB or ^{99m}Tc-MIBI (5μCi/ml) in standard HBSS for 20 min in a humidified incubator (95% O_2, 5% CO_2) at 37°C. Subsequently, hepatocytes were rinsed vigorously twice with 2mL warm standard HBSS or Ca^{2+}-free HBSS (to maintain or disrupt tight junctions, respectively), and incubated with 1.5mL of the same buffer supplemented with chemical inhibitors (100μM MK571 or 20μM GF120918) or vehicle control (0.6% DMSO) for 20min at 37°C. The amount of ^{99m}Tc-MEB or ^{99m}Tc-MIBI in the efflux buffer was sampled at 20min and medium was aspirated. Hepatocytes were lysed as detailed above. Data were normalized to protein concentration in each well, as described above. Samples were analyzed using a gamma counter and corrected for decay.

The amount of substrate was measured in the medium at 20min and in the lysed SCH at the end of the efflux phase. The extent of basolateral and canalicular efflux was determined based on the following equations and normalized to the total substrate mass preloaded in the hepatocytes, which was determined as the sum of the substrate mass in the efflux medium and in the hepatocyte lysate at the end of the efflux phase:

$$\text{Basolateral Efflux} = \text{Total Mass in Efflux Medium}_{\text{Standard HBSS}}$$

$$\text{Apical Efflux} = \text{Total Mass in Efflux Medium}_{Ca^{2+}-\text{free HBSS}} - \text{Total Mass in Efflux Medium}_{\text{Standard HBSS}}$$

Accumulation Studies—The method to determine substrate accumulation in the bile canalicular networks of SCH has been described previously(20, 21). Cells were incubated for 10min at 37°C with 1.5mL of ^{99m}Tc-MIBI (0.5μCi/ml) with or without Bcrp knockdown, and in the presence and absence of 2μM GF120918 in standard buffer. Substrate uptake was corrected for nonspecific binding by subtracting uptake on blank six-well Biocoat™ plates overlaid with Matrigel™. Hepatocytes were lysed as detailed above and data were normalized to protein concentration in each well, as described above.

The biliary excretion index (BEI, %) was calculated using B-CLEAR® technology [Qualyst, Inc., Raleigh, NC; (21)]:

$$\mathrm{BEI}=\frac{\mathrm{Accumulation}_{\mathrm{Cells+Bile}}-\mathrm{Accumulation}_{\mathrm{Cells}}}{\mathrm{Accumulation}_{\mathrm{Cells+Bile}}}\times 100$$

where substrate accumulation in the cells+bile compartments was determined in hepatocytes preincubated for 10 min in standard buffer; cellular accumulation of substrate was determined in hepatocytes preincubated for 10 min with Ca^{2+}-free HBSS.

$$\textit{in vitro}\ \mathrm{Cl}_{\mathrm{biliary}}=\frac{\mathrm{Accumulation}_{\mathrm{Cells+Bile}}-\mathrm{Accumulation}_{\mathrm{Cells}}}{\mathrm{AUC}_{0-T}}$$

where $AUC_{0\text{-}T}$ represents the product of the incubation time (T) and the initial concentration in the medium. *In vitro* $Cl_{biliary}$ values were scaled per kilogram body weight assuming the following: 200 mg protein/g rat liver tissue and 40 g rat liver tissue/kg body weight(22).

RNA Interference (RNAi) Knockdown of Bcrp—The methods for packaging of recombinant siRNA-expressing adenoviral vectors and infection of SCH have been described previously(23). Briefly, after seeding hepatocytes on Biocoat™ plates and changing seeding medium, cells were infected overnight with adenoviral vectors expressing non-target siRNA (siNT), or siRNA targeting the rat Bcrp gene at positions 288–306 (siBcrp) at a multiplicity of infection of 20. Cells were overlaid 24h after seeding, and cultured as described above. Bcrp knockdown was confirmed by Western blot analysis and the *in vitro* $Cl_{biliary}$ of nitrofurantoin was determined using LC/MS/MS analysis, as detailed previously(23).

Statistical Analysis—Statistically significant differences in the efflux data in rat SCH were determined by a two-way analysis of variance for the factors of treatment and route of efflux, which exhibited a significant interaction. Therefore, a one-way ANOVA was performed on basolateral and canalicular efflux data individually for the factor of treatment with Dunnett's post hoc test. A one-way ANOVA was performed on the initial uptake data in suspended hepatocytes with Dunnett's multiple comparisons post hoc test. The criterion for significance in all cases was $p < 0.05$.

Results

Uptake of ^{99m}Tc-MEB, ^{99m}Tc-MIBI, ^{3}H-E217G, and ^{14}C-TEA in Suspended Rat and Human Hepatocytes

Preliminary experiments in suspended rat hepatocytes sampling over 60min indicated that the linear range of uptake was 2.5, 1.5, 2.5, and 5min for ^{99m}Tc-MIBI, ^{99m}Tc-MEB, ^{3}H-E217G, and ^{14}C-TEA, respectively. Therefore, subsequent experiments were conducted up to the respective times to evaluate the initial uptake rate of each substrate. The Oct/OCT inhibitors clonidine, desipramine and decynium 22, and the Oat/OAT inhibitor ketoprofen, and the absence of sodium [substitution with choline-based buffer to rule out the involvement of sodium taurocholate cotransporter (Ntcp/NTCP)] had marginal effects on the initial uptake of ^{99m}Tc-MEB in WT rat and human hepatocytes compared to control (Fig. 1A and 2A). Initial ^{99m}Tc-MEB uptake was significantly reduced to 20.7 and 35.4% of control in the presence of the Oatp/OATP inhibitor rifamycin SV in WT rat and human hepatocytes, respectively (Fig. 1A and 2A). In WT rat hepatocytes, the Oatp inhibitor

glycyrrhizic acid significantly reduced ^{99m}Tc-MEB initial uptake to 39.5% of control (Fig. 1A). Initial ^{99m}Tc-MIBI uptake in suspended WT rat hepatocytes was not influenced by inhibitors or replacement of sodium with choline in the uptake buffer; all values were within 10% of control (Fig. 1B).

In order to confirm the specificity of the selected inhibitors, transport of probe substrates was assessed in the presence of each inhibitor. As expected, initial hepatocyte uptake of the Oatp probe substrate ^{3}H-E217G was inhibited significantly to 15.5 and 23.8% of control in the presence of rifamycin SV and glycyrrhizic acid, respectively, in suspended WT rat hepatoyctes (Fig. 1C), and 51.5% of control in the presence of rifamycin SV in suspended human hepatocytes (Fig. 2B). All other inhibitors had marginal effects on ^{3}H-E217G uptake in both WT rat and human suspended hepatocytes (Fig. 1C and 2B). Initial uptake of the Oct probe substrate ^{14}C-TEA was signficantly inhibited to 23.7% and 25.6% of control in the presence of clonidine and desipramine, respectively, in suspended rat hepatocytes (Fig. 1D), and significantly reduced to 54.2% of control in the presence of decynium 22 (Fig. 2C) in suspended human hepatocytes. Interestingly, the Oatp1a1, Oatp1a4 and Oatp1b2 inhibitor glycyrrhizic acid signficantly reduced ^{14}C-TEA uptake by 62.1% compared to control in suspended rat hepatocytes (Fig. 1D). The uptake of 20 μM ^{3}H-PAH over 60 min was marginally greater than background (data not shown), which was attributed primarily to nonspecific binding to the hepatocytes. ^{3}H-PAH uptake was not significantly influenced by the presence of 50μM MK571 in the incubation medium (a known Mrp inhibitor added to inhibit potential basolateral efflux).

Hepatobiliary Disposition of ^{99m}Tc-MEB in Rat and Human Sandwich-Cultured Hepatocytes—^{99m}Tc-MEB canalicular efflux was slightly lower than basolateral efflux over 20 min in SCH from control WT rats (15.3±5.7% vs. 25.0±6.7% of total preloaded mass; Fig. 3A). In contrast, in human SCH, ^{99m}Tc-MEB canalicular efflux was greater than basolateral efflux (45.8±8.6% vs. 16.7±0.6% of total preloaded mass). ^{99m}Tc-MEB canalicular efflux was ~3-fold greater in human compared to rat SCH, while basolateral efflux in human SCH was slightly lower than in rat SCH (Fig. 3A). ^{99m}Tc-MEB basolateral efflux tended to be higher in TR^{-} SCH (31.8±6.2% of total preloaded mass; Fig. 3A) relative to WT values, while canalicular efflux of ^{99m}Tc-MEB in TR^{-} SCH was negligible (Fig. 3A). MK571 (100μM) decreased ^{99m}Tc-MEB canalicular efflux 85% in rat SCH and 30% in human SCH (Fig. 3A), but increased ^{99m}Tc-MEB basolateral efflux 136% in rat SCH and 240% in human SCH (Fig. 3A). ^{99m}Tc-MEB hepatocellular content (cell only) at the end of the 20-min efflux phase was slightly greater in rat SCH (58.7±7.3%) compared to human SCH (37.6±8.0%) (Table 1), consistent with the species differences observed in the total efflux of ^{99m}Tc-MEB in rat (40.3±5.4%) and human (62.4±8.0%) SCH.

Hepatobiliary Disposition of ^{99m}Tc-MIBI in Rat and Human Sandwich-Cultured Hepatocytes—^{99m}Tc-MIBI basolateral efflux tended to be greater than canalicular efflux over 20 min in SCH from WT rats (40.5±7.6 vs. 23.6±3.4% of total preloaded mass), TR^{-} rats (39.4±7.1 vs. 30.9±2.1% of total preloaded mass), and humans (64.0±4.2 vs. 25.4±6.0% of total preloaded mass) (Fig. 3B). ^{99m}Tc-MIBI canalicular efflux was similar between human and WT rat SCH, but basolateral efflux was 37% greater in human compared to WT rat SCH (Fig. 3B). ^{99m}Tc-MIBI basolateral efflux was similar in SCH from TR^{-} and WT rats; likewise, canalicular efflux of ^{99m}Tc-MIBI was not altered in SCH from TR^{-} compared to WT rats (Fig. 3B). GF120918 (20μM) decreased ^{99m}Tc-MIBI canalicular efflux 1.5-fold in rat SCH and 2.1-fold in human SCH. Interestingly, GF120918 also decreased ^{99m}Tc-MIBI basolateral efflux in rat and human SCH (~2.3- and ~2.9-fold, respectively) (Fig. 3B). Hepatocellular content of ^{99m}Tc-MIBI at the end of the 20-min efflux phase tended to be greater in rat SCH compared to human SCH (Table 1), consistent with greater percent of

total efflux of ^{99m}Tc-MIBI in human (89.4±1.8%) compared to rat (64.0±8.2%) SCH using the 20-min efflux study design.

Using the 10-min accumulation study design, ^{99m}Tc-MIBI accumulation in cells+bile and cells was determined in rat SCH; BEI and *in vitro* $Cl_{biliary}$ values were 18% and 4.07 mL/min/kg, respectively. To examine whether Bcrp and/or P-gp were responsible for the biliary excretion of ^{99m}Tc-MIBI in rat SCH, 10-min accumulation studies were conducted. ^{99m}Tc-MIBI BEI (36.0 and 26.6%) and *in vitro* $Cl_{biliary}$ (8.08 and 9.73mL/min/kg) in day 4 WT rat SCH were increased marginally by infection with adenoviral vectors expressing a non-target control (siNT) or short hairpin RNA targeting rat Bcrp (siBcrp), respectively, compared to noninfected SCH (Fig. 4A). ^{99m}Tc-MIBI BEI and *in vitro* $Cl_{biliary}$ were ablated in the presence of 2μM GF120918 in siNT- and siBcrp-infected SCH, which resulted in a ~2-fold increase in hepatocellular accumulation (cells only) of ^{99m}Tc-MIBI (Fig. 4A). As shown in figure 4B, in day 4 rat SCH, protein levels of Bcrp (normalized by β-actin) in siBcrp-infected cells were ~20% of those in control (siNT-infected) cells. No differences in nitrofurantoin cellular accumulation, BEI, or *in vitro* $Cl_{biliary}$ in noninfected or control siNT-infected rat SCH were noted (Fig. 4C). As expected, the cellular accumulation of nitrofurantoin, a Bcrp substrate, was increased due to the ~6-fold decrease in BEI in siBcrp-infected cells compared to control (siNT-infected) cells.

Discussion

The utility of ^{99m}Tc-MEB and ^{99m}Tc-MIBI as probe substrates for phenotyping the function of specific hepatic transport proteins was confirmed using well-established *in vitro* methods. Suspended hepatocytes and SCH were utilized from rats and humans to characterize hepatic uptake and efflux mechanisms in combination with the use of “specific” chemical inhibitors, as detailed in the methods, to examine the impact of hepatic transport modulation on the disposition of ^{99m}Tc-MEB and ^{99m}Tc-MIBI. Suspended hepatocytes are used primarily to investigate uptake mechanisms; the inability to differentiate between sinusoidal efflux and canalicular excretion limits the utility of suspended hepatocytes for efflux studies (24–26). Isolation of hepatocytes by collagenase digestion and conventional cell culture results in the loss of many liver-specific functions, redistribution of canalicular membrane proteins, loss of cell polarity and architecture including bile canaliculi, and the deterioration of hepatocyte viability within several days (27–29). In contrast, hepatocytes cultured between two layers of gelled collagen (sandwich-cultured configuration) retain more *in vivo*-like properties, including formation of intact canalicular networks and polarized excretory function, and can be used to investigate the hepatobiliary disposition of substrates (21, 30–35).

Model probe substrates [^{3}H-E217G(36, 37); ^{14}C-TEA(38–40); and ^{3}H-PAH(41, 42)] were evaluated in the presence and absence of the panel of inhibitors to confirm the specificity of the selected inhibitors for Oatp/OATP (rifamycin SV and glycyrrhizic acid; Fig. 1C and 2B), Oct/OCT (clonidine, desipramine, and decynium 22; Fig. 1D and 2C) and Oat2/OAT2 (ketoprofen; data not shown), respectively. Unexpectedly, the Oatp/OATP inhibitor glyzyrrhizic acid significantly decreased ^{14}C-TEA initial uptake to 37.9% of control, suggesting that this inhibitor is not specific for Oatp isoforms because TEA is not a substrate of the Oatps expressed in the rat liver(43). Surprisingly, incubation of freshly isolated rat and human hepatocytes with 0.2, 1 or 20μM ^{3}H-PAH over 60min in the absence and presence of 50μM MK571, co-administered to inhibit potential basolateral efflux, resulted in no measurable increase in activity above background. Carrier-mediated retrieval of human OAT1 expressed in *Xenopus* oocytes and HEK293 cells from the cell membrane results in decreased function(44). These findings suggest that Oat2/OAT2 may not be properly localized to assess transport function in freshly isolated rat and human hepatocytes.

Based on the specificity of the chosen inhibitors, ^{99m}Tc-MEB and ^{99m}Tc-MIBI hepatic uptake was examined. ^{99m}Tc-MEB initial uptake was sodium-independent, and was only affected by the Oatp/OATP inhibitors, rifamycin SV and glycyrrhizic acid (Fig. 1A and 2A). These data support the hypothesis that ^{99m}Tc-MEB uptake is predominantly mediated by Oatps/OATPs in rat and human hepatocytes, and is in agreement with data demonstrating ^{99m}Tc-MEB is a substrate of OATP1B1 and OATP1B3 in HEK293 overexpressing cells(3).

^{99m}Tc-MIBI initial uptake in rat hepatocytes was not influenced by inhibitors or the absence of sodium in the uptake buffer (Fig. 1B), suggesting that an active transport process is not involved in ^{99m}Tc-MIBI hepatic uptake at these low concentrations. Concentrations of ^{99m}Tc-MIBI were increased (5 – 200μCi/mL) to saturate a possible active transport process, but partitioning of ^{99m}Tc-MIBI into hepatocytes was linear at designated time points collected for 60min. These findings are consistent with previous reports that ^{99m}Tc-MIBI uptake is a function of free diffusion based on electrical potentials across the plasma and mitochondrial membranes, with localization in the mitochondria by electrostatic forces(45). Therefore, ^{99m}Tc-MIBI uptake experiments were not conducted in suspended human hepatocytes to conserve this limited resource.

Further studies were undertaken to examine the efflux processes involved in ^{99m}Tc-MEB hepatic disposition. Remarkably, the canalicular efflux of ^{99m}Tc-MEB was ~3-fold greater in human compared to WT rat SCH, whereas the basolateral efflux was comparable (Fig. 3A). Based on work by Li et al., total Mrp2/MRP2 protein was not significantly different in day 4 rat and day 7 human SCH (~4fmol/μg protein) utilizing a quantitative LC-MS/MS analysis(46). Thus, the species differences in canalilcular efflux of ^{99m}Tc-MEB observed in the present study cannot be attributed to differences in the absolute amount of Mrp2/MRP2 protein primarily responsible for biliary excretion of ^{99m}Tc-MEB, but could be explained by differences in affinity or maximum velocity, assuming that canalicular efflux is mediated solely by Mrp2/MRP2. ^{99m}Tc-MEB total efflux also was greater in human compared to rat SCH due to this increased canalicular efflux (Fig. 3A). ^{99m}Tc-MEB canalicular efflux was completely ablated in TR$^-$ rat SCH. The Mrp2 inhibitor MK571 decreased ^{99m}Tc-MEB canalicular efflux ~6.7-fold in rat SCH, but only 30% in human SCH (Fig. 3A). This apparent discrepancy could be due to a potential species difference in the hepatic disposition of MK571 leading to lower intracellular exposure of the inhibitor as a result of decreased uptake and/or increased clearance in human hepatocytes. Although species differences in the contribution of P-gp or BCRP to ^{99m}Tc-MEB canalicular efflux in human compared to rat hepatocytes cannot be ruled out, the more likely explanation for these differences may be attributed to limitations in the experimental design of the efflux experiments. During the preloading phase, ^{99m}Tc-MEB accumulates in the canalicular networks and may not be washed away completely before initiating the efflux phase; rapid canalicular excretion of ^{99m}Tc-MEB may occur before MK571 had time to access the hepatocyte and reach the site of MRP2 inhibition, especially in human SCH. Overall, MK571 inhibition and the absence of ^{99m}Tc-MEB in the bile canalicular networks of TR$^-$ rat SCH support the hypothesis that ^{99m}Tc-MEB is a specific Mrp2 probe substrate, consistent with other reports documenting increased hepatic exposure of ^{99m}Tc-MEB in TR$^-$ rats(4), and decreased biliary excretion in patients with Dubin-Johnson syndrome (MRP2-deficiency) administered ^{99m}Tc-MEB analogs(5). ^{99m}Tc-MEB basolateral efflux was increased in TR$^-$ rat SCH compared to WT, and in the presence of MK571 (Fig. 3A), while intracellular accumulation of ^{99m}Tc-MEB was unchanged (Table 1). These important findings suggest that this probe can be redirected from biliary excretion to efflux across the basolateral membrane. This increase in basolateral efflux also could be due, in part, to inhibition of ^{99m}Tc-MEB hepatic re-uptake, because MK571 has been shown to inhibit OATP1B3 with a reported K_i of 0.6μM(47).

Further studies were conducted to investigate the efflux processes involved in ^{99m}Tc-MIBI hepatic disposition. The absence of Mrp2 in TR$^-$ rat SCH did not alter basolateral or canalicular efflux, suggesting that either Mrp2 is not involved, or other proteins (e.g. P-gp) are able to fully compensate (Fig. 3B). In TR$^-$ rats, ^{99m}Tc-MIBI hepatic scintigraphy and biliary excretion were unchanged compared to WT control rats(14). ^{99m}Tc-MIBI efflux was assessed in the presence of 20μM GF120918, a concentration 10-fold greater than previously used to inhibit P-gp in rat SCH(48). This concentration was selected based on studies in cancer cell lines expressing multidrug resistance transport proteins (P-gp and Bcrp) demonstrating GF120918 is a more potent inhibitor of P-gp than Bcrp by an order of magnitude or more (49), and the use of 10 μM GF120918 in isolated perfused rat livers to impair Bcrp-mediated biliary excretion of 4-methylumbelliferyl sulfate generated in the hepatocyte(50). As expected, ^{99m}Tc-MIBI canalicular efflux was GF120918-sensitive, consistent with a role for P-gp and/or Bcrp in ^{99m}Tc-MIBI biliary excretion. Surprisingly, ^{99m}Tc-MIBI basolateral efflux was GF120918-sensitive, suggesting involvement of an active transport process. Hepatocellular accumulation of ^{99m}Tc-MIBI increased in the presence of GF120918 (Table 1) due to decreased basolateral and canalicular efflux of ^{99m}Tc-MIBI (Fig. 3B).

In order to further investigate the transport processes involved in ^{99m}Tc-MIBI biliary excretion, accumulation studies were conducted in rat SCH. The involvement of Bcrp in the biliary excretion of ^{99m}Tc-MIBI was assessed with the use of RNAi knockdown of Bcrp, as confirmed by immunoblot (Fig. 4B), and significantly impaired biliary excretion of the rat Bcrp probe substrate nitrofurantoin (Fig. 4C). This approach using adenoviral vectors expressing a non-target control (siNT) and short hairpin RNA targeting Bcrp (siBcrp) has been shown to efficiently and specifically knock down Bcrp in rat SCH(23). Bcrp knockdown did not affect ^{99m}Tc-MIBI cellular accumulation, biliary excretion or *in vitro* $Cl_{biliary}$ (Fig. 4A). ^{99m}Tc-MIBI biliary excretion was inhibited completely by 2μM GF120918 (Fig. 4A), used previously to inhibit P-gp in rat SCH(48). Cellular accumulation also increased in the presence of GF120918 (Fig. 4A), suggesting that P-gp is the primary protein responsible for the biliary excretion of ^{99m}Tc-MIBI. These findings are in agreement with published *in vitro* data demonstrating the affinity of ^{99m}Tc-MIBI for P-gp in overexpressing cancer cell lines(51, 52) and with human *in vivo* data; ^{99m}Tc-MIBI biliary elimination was reduced and/or hepatic ^{99m}Tc-MIBI retention was increased based on scintigraphy in humans with single nucleotide polymorphisms in the *ABCB1* gene resulting in decreased P-gp function(10), and in cancer patients administered ^{99m}Tc-MIBI and the P-gp inhibitor PSC833(9, 11).

Species differences existed in the fraction of canalicular vs. basolateral efflux of ^{99m}Tc-MEB in rat (38.0% vs. 62.0% of total efflux, respectively) compared to human (73.3% vs. 26.7% of total efflux, respectively; Fig. 3A) SCH. These *in vitro* findings support the clinical observation that biliary clearance is rapid and extensive in humans; ~84% of a 2.3mCi dose of intravenously administered ^{99m}Tc-MEB was recovered in bile in healthy human subjects within 180 min(53). In rats, the biliary excretion profile of ^{99m}Tc-MEB may be more prolonged due to basolateral efflux and subsequent reuptake by hepatocytes; ~95% of a 0.25 mCi dose was recovered in the liver 30 min after intravenous administration(54). In contrast, based on the fraction of canalicular vs. basolateral efflux of ^{99m}Tc-MIBI in rat (36.8% vs. 63.2% of total efflux, respectively) and human (28.3% vs. 71.7% of total efflux, respectively; Fig. 3B) SCH, basolateral excretion of ^{99m}Tc-MIBI appears to be the preferential route of hepatic elimination of this probe in both rats and humans. This finding is consistent with biliary recovery of only ~22% of a 3.1mCi dose of intravenously administered ^{99m}Tc-MIBI in healthy human subjects(55). Overall, the efflux method in SCH is useful for examining the preferential route of hepatic excretion (canalicular vs. basolateral) and elucidating species differences in hepatic efflux.

In summary, the hepatic uptake of ^{99m}Tc-MIBI appears to occur by passive diffusion; ^{99m}Tc-MIBI biliary excretion is mediated by P-gp. ^{99m}Tc-MEB hepatic uptake is predominantly Oatp-mediated with biliary excretion by Mrp2. Species differences exist between rat and human in the total efflux and route of efflux for ^{99m}Tc-MEB. Preloading SCH and measurement of efflux over 20min in SCH is a useful approach to investigate the route of hepatic excretion (basolateral vs. canalicular), species differences in basolateral and canalicular efflux, and compensatory changes in canalicular and basolateral efflux due to impaired transport function associated with drug interactions, disease state alterations or genetic variation.

Acknowledgments

This research was supported by a grant from the National Institutes of Health (R01GM41935). Brandon Swift was supported by an Eli Lilly and Company Foundation predoctoral fellowship. The authors would like to thank Arlene S. Bridges, Ph.D., for her analytical support, Yiwei Rong, for her technical expertise in the isolation of rat hepatocytes, and CellzDirect, Life Technologies, for kindly providing freshly isolated suspended and sandwich-cultured human hepatocytes.

Abbreviations Used

^{99m}Tc-MEB	^{99m}Technetium-mebrofenin
^{99m}Tc-MIBI	^{99m}Technetium-sestamibi
SCH	sandwich-cultured hepatocytes
WT	wild-type
P-gp	multidrug resistance protein P-glycoprotein
Bcrp	breast cancer resistance protein
Mrp	multidrug resistance-associated protein
siBcrp	RNAi short hairpin knockdown of rat Bcrp
BEI	biliary excretion index
$Cl_{biliary}$	*in vitro* biliary clearance
DMEM	Dulbecco's modified Eagle's medium
E217G	estradiol-17-β-D-glucuronide
PAH	para-aminohippuric acid
TEA	tetraethylammonium
FBS	fetal bovine serum
HBSS	Hanks' balanced salt solution
GF120918	N-(4-[2-(1,2,3,4-tetrahydro-6,7-dimethoxy-2-isoquinolinyl)ethyl]-phenyl)-9,10-dihydro-5-methoxy-9-oxo-4-acridine carboxamide
OCT	organic cation transporter
OAT	organic anion transporter
siNT	non-target siRNA
NTCP	sodium taurocholate cotransporter

References

1. Doo E, Krishnamurthy GT, Eklem MJ, Gilbert S, Brown PH. Quantification of hepatobiliary function as an integral part of imaging with technetium-99m-mebrofenin in health and disease. J Nucl Med. 1991; 32:48–57. [PubMed: 1988637]
2. Krishnamurthy GT, Turner FE. Pharmacokinetics and clinical application of technetium 99m-labeled hepatobiliary agents. Semin Nucl Med. 1990; 20:130–49. [PubMed: 2184521]
3. Ghibellini G, Leslie EM, Pollack GM, Brouwer KL. Use of tc-99m mebrofenin as a clinical probe to assess altered hepatobiliary transport: integration of in vitro, pharmacokinetic modeling, and simulation studies. Pharm Res. 2008; 25:1851–60. [PubMed: 18509604]
4. Bhargava KK, Joseph B, Ananthanarayanan M, Balasubramaniyan N, Tronco GG, Palestro CJ, Gupta S. Adenosine triphosphate-binding cassette subfamily C member 2 is the major transporter of the hepatobiliary imaging agent (99m)Tc-mebrofenin. J Nucl Med. 2009; 50:1140–6. [PubMed: 19525466]
5. Pinos T, Constansa JM, Palacin A, Figueras C. A new diagnostic approach to the Dubin-Johnson syndrome. Am J Gastroenterol. 1990; 85:91–3. [PubMed: 2296972]
6. Beller GA, Sinusas AJ. Experimental studies of the physiologic properties of technetium-99m isonitriles. Am J Cardiol. 1990; 66:5E–8E.
7. Mobasseri S, Hendel RC. Cardiac imaging in women: use of radionuclide myocardial perfusion imaging and echocardiography for acute chest pain. Cardiol Rev. 2002; 10:149–60. [PubMed: 12047793]
8. Piwnica-Worms D, Chiu ML, Budding M, Kronauge JF, Kramer RA, Croop JM. Functional imaging of multidrug-resistant P-glycoprotein with an organotechnetium complex. Cancer Res. 1993; 53:977–84. [PubMed: 8094997]
9. Luker GD, Fracasso PM, Dobkin J, Piwnica-Worms D. Modulation of the multidrug resistance P-glycoprotein: detection with technetium-99m-sestamibi in vivo. J Nucl Med. 1997; 38:369–72. [PubMed: 9074520]
10. Wong M, Evans S, Rivory LP, Hoskins JM, Mann GJ, Farlow D, Clarke CL, Balleine RL, Gurney H. Hepatic technetium Tc 99m-labeled sestamibi elimination rate and ABCB1 (MDR1) genotype as indicators of ABCB1 (P-glycoprotein) activity in patients with cancer. Clin Pharmacol Ther. 2005; 77:33–42. [PubMed: 15637529]
11. Chen CC, Meadows B, Regis J, Kalafsky G, Fojo T, Carrasquillo JA, Bates SE. Detection of in vivo P-glycoprotein inhibition by PSC 833 using Tc-99m sestamibi. Clin Cancer Res. 1997; 3:545–52. [PubMed: 9815718]
12. Slapak CA, Dahlheimer J, Piwnica-Worms D. Reversal of multidrug resistance with LY335979: functional analysis of P-glycoprotein-mediated transport activity and its modulation in vivo. J Clin Pharmacol. 2001; (Suppl):29S–38S. [PubMed: 11452726]
13. Hendrikse NH, Franssen EJ, van der Graaf WT, Meijer C, Piers DA, Vaalburg W, de Vries EG. 99mTc-sestamibi is a substrate for P-glycoprotein and the multidrug resistance-associated protein. Br J Cancer. 1998; 77:353–8. [PubMed: 9472628]
14. Hendrikse NH, Kuipers F, Meijer C, Havinga R, Bijleveld CM, van der Graaf WT, Vaalburg W, de Vries EG. In vivo imaging of hepatobiliary transport function mediated by multidrug resistance associated protein and P-glycoprotein. Cancer Chemother Pharmacol. 2004; 54:131–8. [PubMed: 15118837]
15. Michael M, Thompson M, Hicks RJ, Mitchell PL, Ellis A, Milner AD, Di Iulio J, Scott AM, Gurtler V, Hoskins JM, Clarke SJ, Tebbut NC, Foo K, Jefford M, Zalcberg JR. Relationship of hepatic functional imaging to irinotecan pharmacokinetics and genetic parameters of drug elimination. J Clin Oncol. 2006; 24:4228–35. [PubMed: 16896007]
16. Wong M, Balleine RL, Blair EY, McLachlan AJ, Ackland SP, Garg MB, Evans S, Farlow D, Collins M, Rivory LP, Hoskins JM, Mann GJ, Clarke CL, Gurney H. Predictors of vinorelbine pharmacokinetics and pharmacodynamics in patients with cancer. J Clin Oncol. 2006; 24:2448–55. [PubMed: 16651648]
17. LeCluyse EL, Bullock PL, Parkinson A, Hochman JH. Cultured rat hepatocytes. Pharm Biotechnol. 1996; 8:121–59. [PubMed: 8791809]

18. Leslie EM, Watkins PB, Kim RB, Brouwer KL. Differential inhibition of rat and human Na+-dependent taurocholate cotransporting polypeptide (NTCP/SLC10A1)by bosentan: a mechanism for species differences in hepatotoxicity. J Pharmacol Exp Ther. 2007; 321:1170–8. [PubMed: 17374746]
19. Baur H, Kasperek S, Pfaff E. Criteria of viability of isolated liver cells. Hoppe Seylers Z Physiol Chem. 1975; 356:827–38. [PubMed: 241693]
20. Wolf KK, Brouwer KR, Pollack GM, Brouwer KL. Effect of albumin on the biliary clearance of compounds in sandwich-cultured rat hepatocytes. Drug Metab Dispos. 2008; 36:2086–92. [PubMed: 18653747]
21. Liu X, LeCluyse EL, Brouwer KR, Gan LS, Lemasters JJ, Stieger B, Meier PJ, Brouwer KL. Biliary excretion in primary rat hepatocytes cultured in a collagen-sandwich configuration. Am J Physiol. 1999; 277:G12–21. [PubMed: 10409146]
22. Seglen PO. Preparation of isolated rat liver cells. Methods Cell Biol. 1976; 13:29–83. [PubMed: 177845]
23. Yue W, Abe K, Brouwer KL. Knocking Down Breast Cancer Resistance Protein (Bcrp) by Adenoviral Vector-Mediated RNA Interference (RNAi) in Sandwich-Cultured Rat Hepatocytes: A Novel Tool To Assess the Contribution of Bcrp to Drug Biliary Excretion. Mol Pharm. 2009; 6:134–43. [PubMed: 19105722]
24. Oude Elferink RP, Ottenhoff R, Liefting WG, Schoemaker B, Groen AK, Jansen PL. ATP-dependent efflux of GSSG and GS-conjugate from isolated rat hepatocytes. Am J Physiol. 1990; 258:G699–706. [PubMed: 2333997]
25. Studenberg SD, Brouwer KL. Effect of phenobarbital and p-hydroxyphenobarbital glucuronide on acetaminophen metabolites in isolated rat hepatocytes: use of a kinetic model to examine the rates of formation and egress. J Pharmacokinet Biopharm. 1993; 21:175–94. [PubMed: 8229679]
26. Tarao K, Olinger EJ, Ostrow JD, Balistreri WF. Impaired bile acid efflux from hepatocytes isolated from the liver of rats with cholestasis. Am J Physiol. 1982; 243:G253–8. [PubMed: 7124954]
27. Groothuis GM, Hulstaert CE, Kalicharan D, Hardonk MJ. Plasma membrane specialization and intracellular polarity of freshly isolated rat hepatocytes. Eur J Cell Biol. 1981; 26:43–51. [PubMed: 6276181]
28. Borlak J, Klutcka T. Expression of basolateral and canalicular transporters in rat liver and cultures of primary hepatocytes. Xenobiotica. 2004; 34:935–47. [PubMed: 15801539]
29. Luttringer O, Theil FP, Lave T, Wernli-Kuratli K, Guentert TW, de Saizieu A. Influence of isolation procedure, extracellular matrix and dexamethasone on the regulation of membrane transporters gene expression in rat hepatocytes. Biochem Pharmacol. 2002; 64:1637–50. [PubMed: 12429353]
30. Dunn JC, Tompkins RG, Yarmush ML. Hepatocytes in collagen sandwich: evidence for transcriptional and translational regulation. J Cell Biol. 1992; 116:1043–53. [PubMed: 1734019]
31. Dunn JC, Yarmush ML, Koebe HG, Tompkins RG. Hepatocyte function and extracellular matrix geometry: long-term culture in a sandwich configuration. Faseb J. 1989; 3:174–7. [PubMed: 2914628]
32. Dunn JC, Tompkins RG, Yarmush ML. Long-term in vitro function of adult hepatocytes in a collagen sandwich configuration. Biotechnol Prog. 1991; 7:237–45. [PubMed: 1367596]
33. LeCluyse EL, Audus KL, Hochman JH. Formation of extensive canalicular networks by rat hepatocytes cultured in collagen-sandwich configuration. Am J Physiol. 1994; 266:C1764–74. [PubMed: 8023906]
34. Liu X, Brouwer KL, Gan LS, Brouwer KR, Stieger B, Meier PJ, Audus KL, LeCluyse EL. Partial maintenance of taurocholate uptake by adult rat hepatocytes cultured in a collagen sandwich configuration. Pharm Res. 1998; 15:1533–9. [PubMed: 9794494]
35. Liu X, LeCluyse EL, Brouwer KR, Lightfoot RM, Lee JI, Brouwer KL. Use of Ca2+ modulation to evaluate biliary excretion in sandwich-cultured rat hepatocytes. J Pharmacol Exp Ther. 1999; 289:1592–9. [PubMed: 10336557]
36. Brock WJ, Vore M. Characterization of uptake of steroid glucuronides into isolated male and female rat hepatocytes. J Pharmacol Exp Ther. 1984; 229:175–81. [PubMed: 6707932]

37. Shitara Y, Li AP, Kato Y, Lu C, Ito K, Itoh T, Sugiyama Y. Function of uptake transporters for taurocholate and estradiol 17beta-D-glucuronide in cryopreserved human hepatocytes. Drug Metab Pharmacokinet. 2003; 18:33–41. [PubMed: 15618717]

38. Busch AE, Quester S, Ulzheimer JC, Waldegger S, Gorboulev V, Arndt P, Lang F, Koepsell H. Electrogenic properties and substrate specificity of the polyspecific rat cation transporter rOCT1. J Biol Chem. 1996; 271:32599–604. [PubMed: 8955087]

39. Chen R, Nelson JA. Role of organic cation transporters in the renal secretion of nucleosides. Biochem Pharmacol. 2000; 60:215–9. [PubMed: 10825466]

40. Grundemann D, Gorboulev V, Gambaryan S, Veyhl M, Koepsell H. Drug excretion mediated by a new prototype of polyspecific transporter. Nature. 1994; 372:549–52. [PubMed: 7990927]

41. Kobayashi Y, Ohshiro N, Sakai R, Ohbayashi M, Kohyama N, Yamamoto T. Transport mechanism and substrate specificity of human organic anion transporter 2 (hOat2 [SLC22A7]). J Pharm Pharmacol. 2005; 57:573–8. [PubMed: 15901346]

42. Sekine T, Cha SH, Tsuda M, Apiwattanakul N, Nakajima N, Kanai Y, Endou H. Identification of multispecific organic anion transporter 2 expressed predominantly in the liver. FEBS Lett. 1998; 429:179–82. [PubMed: 9650585]

43. Cattori V, van Montfoort JE, Stieger B, Landmann L, Meijer DK, Winterhalter KH, Meier PJ, Hagenbuch B. Localization of organic anion transporting polypeptide 4 (Oatp4) in rat liver and comparison of its substrate specificity with Oatp1, Oatp2 and Oatp3. Pflugers Arch. 2001; 443:188–95. [PubMed: 11713643]

44. Wolff NA, Thies K, Kuhnke N, Reid G, Friedrich B, Lang F, Burckhardt G. Protein kinase C activation downregulates human organic anion transporter 1-mediated transport through carrier internalization. J Am Soc Nephrol. 2003; 14:1959–68. [PubMed: 12874449]

45. Chiu ML, Kronauge JF, Piwnica-Worms D. Effect of mitochondrial and plasma membrane potentials on accumulation of hexakis (2-methoxyisobutylisonitrile) technetium(I) in cultured mouse fibroblasts. J Nucl Med. 1990; 31:1646–53. [PubMed: 2213187]

46. Li N, Bi YA, Duignan DB, Lai Y. Quantitative expression profile of hepatobiliary transporters in sandwich cultured rat and human hepatocytes. Mol Pharm. 2009; 6:1180–9. [PubMed: 19545175]

47. Letschert K, Komatsu M, Hummel-Eisenbeiss J, Keppler D. Vectorial transport of the peptide CCK-8 by double-transfected MDCKII cells stably expressing the organic anion transporter OATP1B3 (OATP8) and the export pump ABCC2. J Pharmacol Exp Ther. 2005; 313:549–56. [PubMed: 15665139]

48. Annaert PP, Turncliff RZ, Booth CL, Thakker DR, Brouwer KL. P-glycoprotein-mediated in vitro biliary excretion in sandwich-cultured rat hepatocytes. Drug Metab Dispos. 2001; 29:1277–83. [PubMed: 11560870]

49. de Bruin M, Miyake K, Litman T, Robey R, Bates SE. Reversal of resistance by GF120918 in cell lines expressing the ABC half-transporter, MXR. Cancer Lett. 1999; 146:117–26. [PubMed: 10656616]

50. Zamek-Gliszczynski MJ, Hoffmaster KA, Humphreys JE, Tian X, Nezasa K, Brouwer KL. Differential involvement of Mrp2 (Abcc2) and Bcrp (Abcg2) in biliary excretion of 4-methylumbelliferyl glucuronide and sulfate in the rat. J Pharmacol Exp Ther. 2006; 319:459–67. [PubMed: 16857726]

51. Ballinger JR, Hua HA, Berry BW, Firby P, Boxen I. 99Tcm-sestamibi as an agent for imaging P-glycoprotein-mediated multi-drug resistance: in vitro and in vivo studies in a rat breast tumour cell line and its doxorubicin-resistant variant. Nucl Med Commun. 1995; 16:253–7. [PubMed: 7624105]

52. Rao VV, Chiu ML, Kronauge JF, Piwnica-Worms D. Expression of recombinant human multidrug resistance P-glycoprotein in insect cells confers decreased accumulation of technetium-99m-sestamibi. J Nucl Med. 1994; 35:510–5. [PubMed: 7906729]

53. Ghibellini G, Johnson BM, Kowalsky RJ, Heizer WD, Brouwer KL. A novel method for the determination of biliary clearance in humans. Aaps J. 2004; 6:e33. [PubMed: 15760098]

54. Nunn AD, Loberg MD, Conley RA. A structure-distribution-relationship approach leading to the development of Tc-99m mebrofenin: an improved cholescintigraphic agent. J Nucl Med. 1983; 24:423–30. [PubMed: 6842291]

55. Ghibellini G, Vasist LS, Leslie EM, Heizer WD, Kowalsky RJ, Calvo BF, Brouwer KL. In vitro-in vivo correlation of hepatobiliary drug clearance in humans. Clin Pharmacol Ther. 2007; 81:406–13. [PubMed: 17235333]

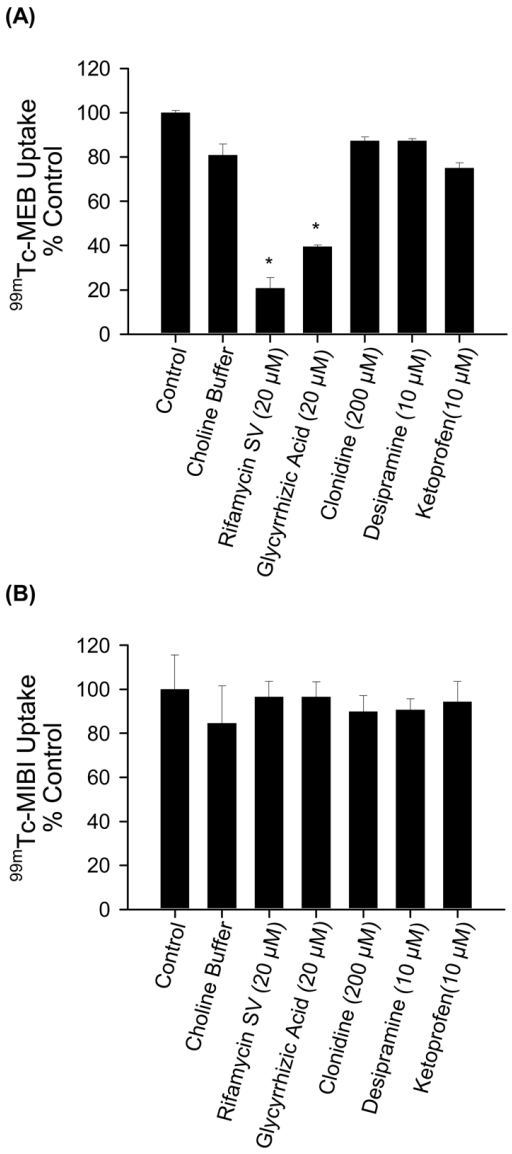

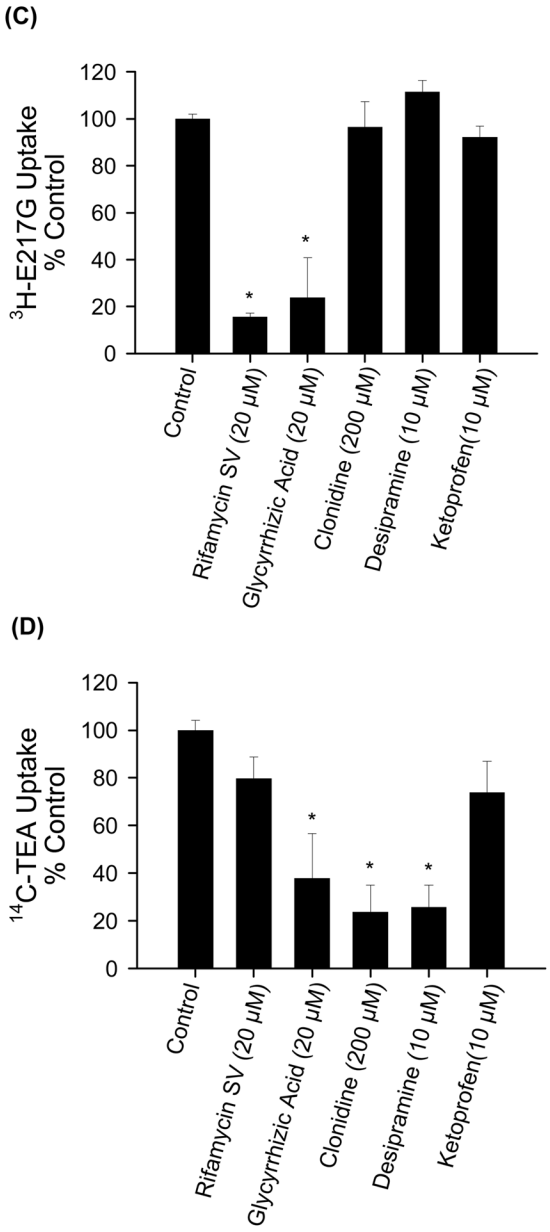

FIGURE 1.

Initial uptake rate of (A) ^{99m}Tc-MEB (5μCi/mL), (B) ^{99m}Tc-MIBI (5μCi/mL), (C) ^{3}H-E217G (1μM), and (D) ^{14}C-TEA (20μM) in suspended WT rat hepatocytes in the absence and presence of transport protein inhibitors (mean percentage ± SEM; n=3 livers per group, in duplicate or triplicate); *, $p<0.05$ versus control.

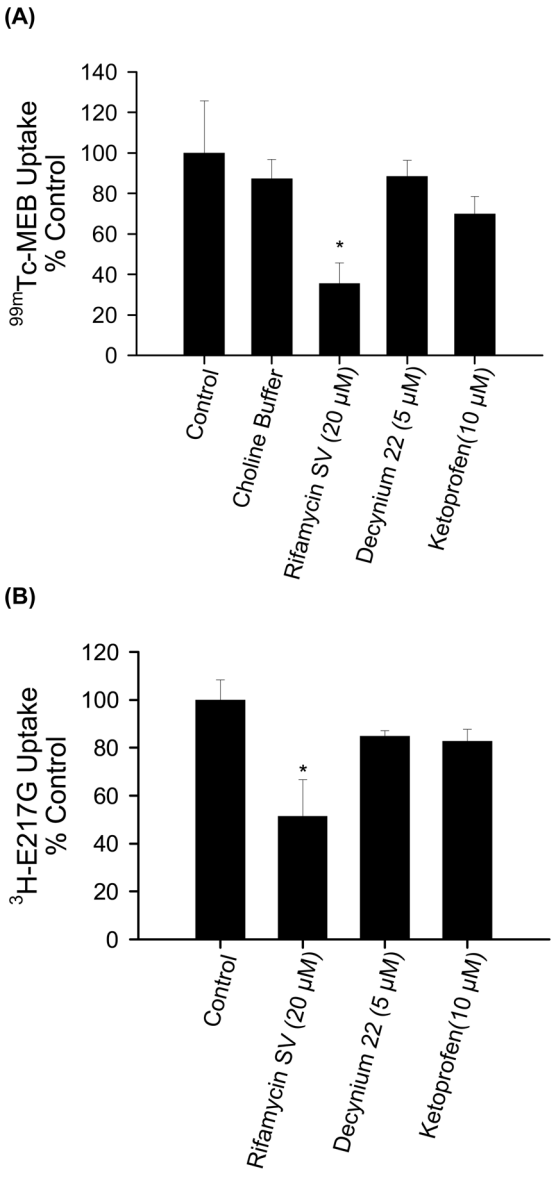

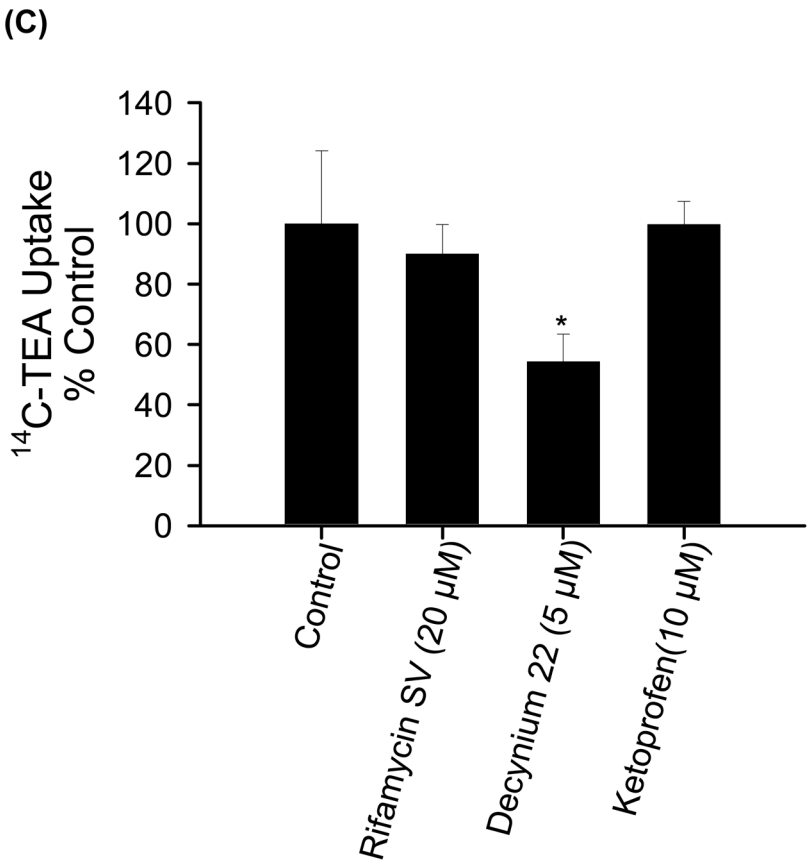

FIGURE 2.

Initial uptake rate of (A) ^{99m}Tc-MEB (5μCi/mL), (B) ^{3}H-E217G (1μM), and (C) ^{14}C-TEA (20μM) in suspended human hepatocytes in the absence and presence of transport protein inhibitors (mean percentage ± SEM; n=3 livers per group, in duplicate or triplicate); *, $p<0.05$ versus control.

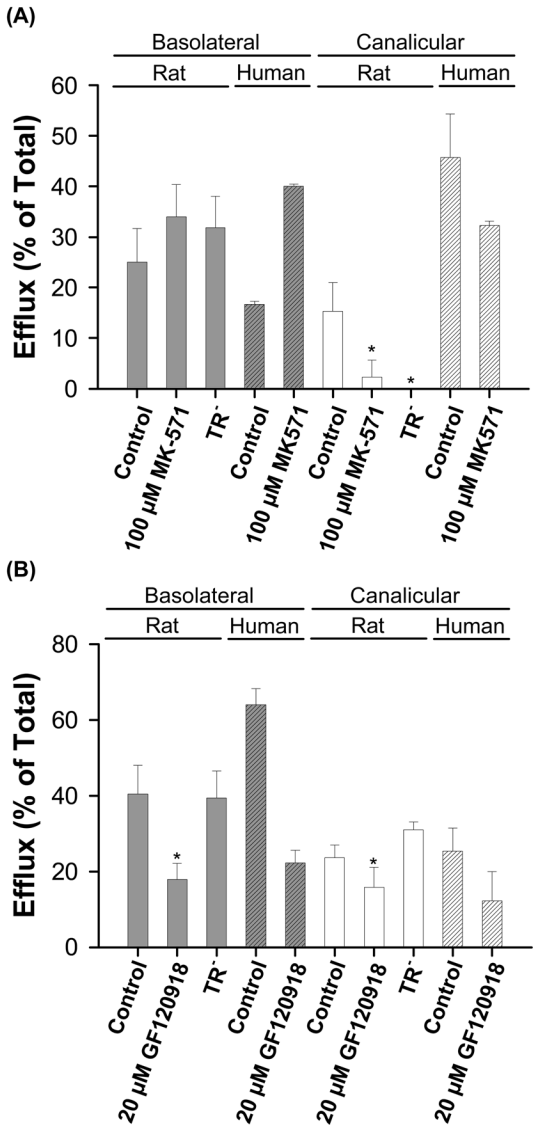

FIGURE 3.

^{99m}Tc-MEB (A) and ^{99m}Tc-MIBI (B) basolateral (dark grey bars) and canalicular (white bars) efflux over 20 min (5µCi/mL, 20min preload) in day 4 rat (WT and TR^{-}) and day 7 human (hatched) sandwich-cultured hepatocytes. Data were obtained after a 20-min efflux phase in incubation medium containing standard (basolateral) or Ca^{+}-free (basolateral + canalicular) HBSS (mean ± SEM or Range; n=4 WT rat livers, n=3 TR^{-} rat livers and n=2 human livers in triplicate; statistical analysis was performed on rat sandwich-cultured hepatocyte data only), *, $p<0.05$ versus control.

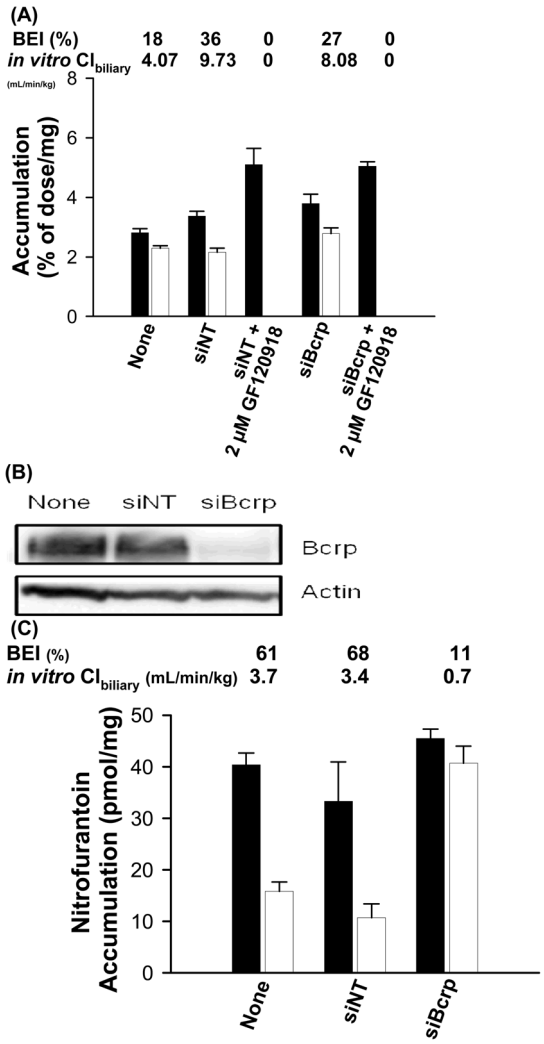

FIGURE 4.

^{99m}Tc-MIBI (A) accumulation in cells+bile (black bars) and cells (white bars), biliary excretion index (BEI) and *in vitro* $Cl_{biliary}$ determined after a 10-min incubation with 0.5 μCi/mL ^{99m}Tc-MIBI in day 4 WT sandwich-cultured rat hepatocytes non-infected or infected with adenoviral vectors expressing short hairpin RNA targeting rat Bcrp (siBcrp) or a non-target control (siNT) (representative data; mean ± SD; n=3 livers). Bcrp (B) expression in day 4 non-infected (None) or sandwich-cultured rat hepatocytes infected with adenoviral vectors siNT and siBcrp. Representative results are shown with β-actin as the loading control. Nitrofurantoin (C) accumulation in cells+bile (black bars) and cells (white bars), BEI and *in vitro* $Cl_{biliary}$ were determined after a 10-min incubation with 5 μM nitrofurantoin in day 4 WT sandwich-cultured rat hepatocytes non-infected or infected with siBcrp or siNT (representative data; mean ± SD).

TABLE I

^{99m}Tc-MEB and ^{99m}Tc-MIBI hepatocellular content in cell lysate at the end of the 20-min efflux experiment in day 4 rat (WT and TR$^-$) and day 7 human sandwich-cultured hepatocytes expressed as a percent of the total substrate mass preloaded in the hepatocytes (mean ± SEM or Range; n=4 WT rat livers, n=3 TR$^-$ rat livers and n=2 human livers in triplicate; Inhibitor = 100μM MK571 for ^{99m}Tc-MEB and 20μM GF120918 for ^{99m}Tc-MIBI).

	Rat			Human	
	Control	**Inhibitor**	**TR$^-$**	**Control**	**Inhibitor**
^{99m}Tc-MEB	58.7 ± 7.3	63.4 ± 4.8	78.8 ± 13.2	37.6 ± 8.0	27.7 ± 0.4
^{99m}Tc-MIBI	34.0 ± 4.3	64.6 ± 6.6	29.7 ± 5.4	10.6 ± 1.8	65.5 ± 11.1